Drainage development on basaltic lava flows, Cima volcanic field, southeast California, and Lunar Crater volcanic field, south-central Nevada

JOHN C. DOHRENWEND *U.S. Geological Survey, 345 Middlefield Road, Menlo Park, California 94025*
ATHOL D. ABRAHAMS *Department of Geography, State University of New York at Buffalo, Buffalo, New York 14260*
BRENT D. TURRIN *U.S. Geological Survey, 345 Middlefield Road, Menlo Park, California 94025*

ABSTRACT

Drainage networks on the accretionary eolian mantles of 11 K-Ar-dated lava flows in the Cima volcanic field and 8 K-Ar-dated flows in the Lunar Crater volcanic field show several related and progressive changes with flow age. If it is assumed that these changes with flow age reflect changes through time, they provide a useful perspective on the early stages of drainage-network development. These drainage networks grow in a manner that is consistent with the qualitative model proposed by Glock. After accumulation of an eolian mantle (requiring 0.1 to 0.2 m.y.), master drainages extend to all parts of a flow. During this period of elongation, which lasts for ~0.2 to 0.3 m.y., drainage density (D) and link frequency (F) increase rapidly whereas the value of Shreve's kappa (κ) declines. After ~0.4 m.y., elaboration replaces elongation as the principal mode of network extension and remains predominant throughout the remainder of the 1.1-m.y. period of record. Elaboration proceeds mainly by the formation of short tributaries along existing streams and by the creation of short streams along flow margins. During the early phases of elaboration, D and F attain a condition wherein the number and lengths of channel links are approximately adjusted to one another, and κ reaches a minimum value of ~0.75. Thereafter, the continuing addition of short tributaries to existing streams causes D, F, and κ to increase slowly as the networks evolve toward maximum extension.

INTRODUCTION

The changing form of landscapes with time is a subject that has long been a primary focus of geomorphology, and central to the subject of landscape change is the question of drainage-network evolution. Fluvial erosion is one of the primary agents of landscape degradation, and drainage-network development is one of the more conspicuous and informative products of fluvial erosion.

Because the time required to effect significant change in most full-sized landscapes is long relative to the time available to the observer, the study of landscape change must, of necessity, be approached indirectly. In the specific case of drainage-network evolution, a variety of approaches have been employed. These include (1) direct observation and measurement of morphologic changes in small areas of rapid erosion (Schumm, 1956; Morisawa, 1964), (2) experimental modeling using readily erodible materials and artificially induced water flow (Parker and Schumm, 1982; Schumm, 1977), (3) simulation modeling using stochastic techniques (for example, Leopold and Langbein, 1962; Smart and others, 1967; Howard, 1971), (4) comparison of full-scale landforms or landscapes arranged in inferred erosional sequences and assuming that such changes in space are representative of changes through time (Glock, 1931; Melton, 1958a), and (5) comparison of full-scale landforms or landscapes of known age selected from near-uniform environments (where climatic, tectonic, lithologic, and base-level influences vary within relatively narrow limits) and arranged in temporal sequences (Ruhe, 1952; Leopold and others, 1964, p. 423–426; Wells and others, 1985).

A number of significant relations have been defined by these various approaches. By comparing several drainage basins arranged in a presumed erosional sequence, Glock (1931) defined a qualitative sequence of drainage-network development: initiation, extension by elongation (the headward growth of new streams), extension by elaboration (the addition of tributaries), maximum extension, and integration (network simplification by abstraction of tributaries and progressive piracy). Refinements to this qualitative sequence have recently been suggested by experimental study of channel network development in an artificial 140-m^2 drainage basin (Parker, 1977; Parker and Schumm, 1982). In these experiments, the mode of network development was apparently determined by initial conditions. When a network develops on a relatively steep slope without base-level lowering, it appears to follow the Glock model of rapid initial elongation of master streams followed by elaboration as the addition of tributaries fills out the network. Alternatively, when a network develops on a gently inclined surface with base-level lowering, it grows headward in a fully elaborated state.

Ruhe (1952) documented progressive differences between channel networks on several ages of Pleistocene till in central Iowa. Leopold and others (1964, p. 423–426) measured drainage densities (total channel length per unit area) and stream frequencies (total number of Strahler streams per unit area) for representative examples of these networks and plotted these network parameters against the approximate ages of the subjacent tills. Both drainage density (D) and stream frequency (Fs) increased rapidly until 17,000 yr and then increased progressively more slowly as they approached equilibrium values. Throughout the development of these networks, D increased more slowly than did Fs, and the relation between D and Fs approximated $Fs \propto D^2$.

Melton (1958a) obtained a similar expression

$$Fs = 0.694\ D^2 \qquad (1)$$

from a regression analysis of Fs against D for 156 mature drainage basins of diverse size and environment. The high coefficient of determination ($r^2 = 0.94$) for this regression demonstrates the constancy of the dimensionless ratio Fs/D^2 for mature drainage basins, and, as Melton rec-

Geological Society of America Bulletin, v. 99, p. 405–413, 11 figs., 2 tables, September 1987.

ognized, this constancy is indicative of a fundamental adjustment between the number and length of channels in a mature drainage network. He termed this ratio the "relative density" and described it as a "scale-free measure of the (in)completeness with which the channel net fills the basin outline for a given number of channel segments" (Melton, 1958b, p. 446–447).

Shreve (1967) provided further insight into the behavior of Fs/D^2 by reducing this ratio to more elementary morphological terms. Defining the quantity

$$\kappa = F/D^2, \quad (2)$$

where F is the link frequency (total number of channel links per unit area), he showed that if $\kappa = 1$,

$$Fs/D^2 \simeq 2/3 \quad (3)$$

for large, topologically random channel networks. This result, which is essentially the same as equation 1, shows that the fundamental adjustment to which Melton referred is more simply and elegantly expressed by the quantity κ than by the ratio Fs/D^2. Moreover, it implies that channel networks adjust in such a manner as to approximately maintain the equality

$$F = D^2. \quad (4)$$

In this paper, we investigate the development of drainage networks on a series of K-Ar–dated basaltic lava flows in the Cima and Lunar Crater volcanic fields of the southwest Basin and Range. These lava flows, which range in age from 0.015 Ma to as old as 1.09 Ma, are veneered by 1- to 3-m-thick eolian mantles of silt and fine sand. The drainage networks developed on these eolian mantles represent the initiation and extension phases of Glock's (1931) developmental sequence and provide a unique opportunity to analyze the early development of full-scale drainage networks.

LAVA-FLOW SURFACES AT THE CIMA AND LUNAR CRATER VOLCANIC FIELDS

Quaternary volcanic fields are numerous and widely distributed across the southwestern United States (Luedke and Smith, 1978, 1981). Two of these fields were selected for detailed study of drainage development on lava-flow surfaces, the Cima volcanic field in the eastern Mojave Desert and the Lunar Crater volcanic field of the southern Great Basin (Fig. 1). Several factors combine to make these fields ideal areas for the study of drainage development through time. (1) Both fields contain large numbers of basaltic lava flows, which are in many cases widely spaced so that interactions between flows have been minimized. (2) Flows in both fields have been emplaced on relatively undissected, uniformly sloping piedmonts that have been either stable surfaces of fluvial transport or gradually downwasting surfaces of fluvial erosion during most or all of Quaternary time (Dohrenwend and others, 1984a, 1984b; Turrin and Dohrenwend, 1984). (3) Both fields are in relatively stable tectonic environments with little or no Quaternary uplift or tilting (Dohrenwend and others, 1984b; Turrin and Dohrenwend, 1984). (4) Both fields are situated in arid continental environments with 11 to 16 °C mean annual temperatures and 10 to 15 cm mean annual precipitation. (5) Finally, both fields are fairly well dated, with 41 K-Ar dates on Quaternary flows in the Cima field (Dohrenwend and others, 1984a; Turrin and others, 1985) and 12 K-Ar dates on Quaternary flows in the Lunar Crater field (Turrin and Dohrenwend, 1984). Consequently, these fields contain numerous lava flows of known age and for which most influences on surficial geomorphic processes have been constrained between narrow limits so that the drainage networks on these flows can be directly compared as a means of investigating the systematic changes that occur in such networks as they develop through time.

Cima Volcanic Field

The Cima volcanic field, in the eastern Mojave Desert ~120 km southwest of Las Vegas, contains 32 Quaternary vents and ~50 Quaternary lava flows that range in composition from alkali olivine basalt to basanite. These cones and flows range from ~0.015 to 1.09 m.y. old, and volcanic activity has been relatively uniformly distributed throughout this period (Dohrenwend and others, 1984a; Turrin and others, 1985). The flows, as much as 9.1 km long and 1.7 km wide, form a morphologic continuum between two distinct types. Elongate flows are characterized by average length-to-width (L/W) ratios generally >4, by mean surface gradients generally <5%, and by flow thicknesses that typically range between 2.5 and 4.0 m. Most of the elongate flows that are suitable for drainage network analysis are relatively small (<1 km^2 in area and 0.5 km in average width). Equant flows are characterized by L/W ratios <3, by mean sur-

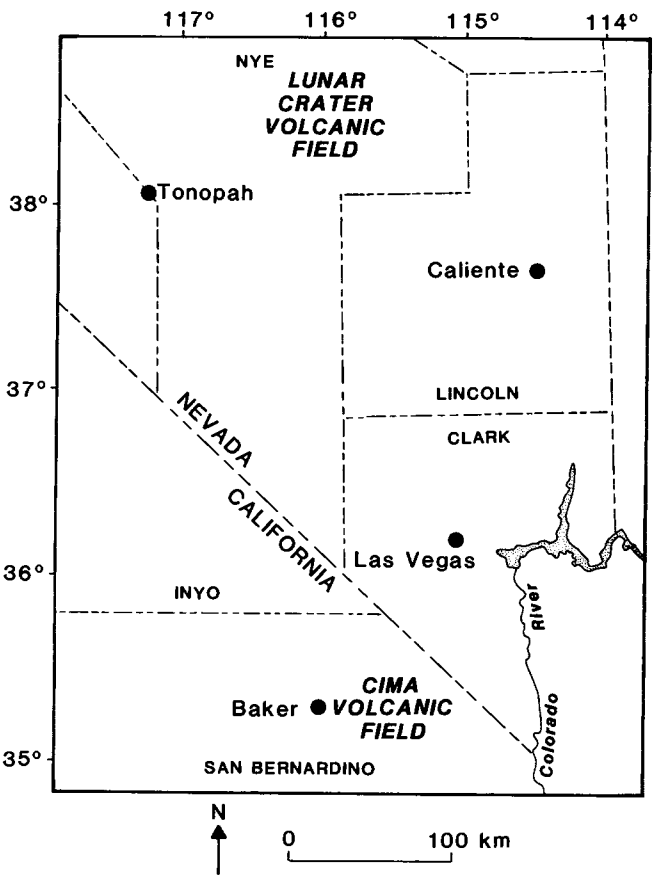

Figure 1. Locations of the Cima volcanic field, eastern Mojave Desert, California, and of the Lunar Crater volcanic field, south-central Nevada.

face gradients of 4% to 8%, and by flow thicknesses of as much as 30 m in some areas. Equant flows suitable for drainage analysis range in size from 0.6 to 2.05 km^2.

The climate of the Cima area is arid and hot. Estimates, based on extrapolations from a 12-yr record at Silver Lake 30 km to the northwest (U.S. Department of Commerce, 1955), indicate a mean annual temperature of 15 to 17 °C, a mean minimum January temperature of 0 °C, and a mean maximum July temperature of 37 °C. Mean annual precipitation is ~10 to 20 cm. Nearly half of this precipitation occurs during winter frontal storms, and ~30% falls during late summer convection storms. During the full-glacial late Pleistocene, summer precipitation was probably less than at present, winter precipitation was probably greater, and summer temperatures were almost certainly less than present summer temperatures (Spaulding and others, 1983). Vegetation on the Cima lava flows is sparse; the Mojave Desert scrub community is dominant below 1,250 m, and Joshua tree woodland is dominant at higher elevations (Vasek and Barbour, 1977).

Lunar Crater Volcanic Field

The Lunar Crater volcanic field, in the south-central Great Basin ~100 km east-northeast of Tonopah, Nevada, and 230 km north of Las Vegas, contains ~100 Quaternary vents and at least 35 Quaternary flows arranged in a northeast-trending zone that extends obliquely across the west piedmont and crest of the Pancake Range. These basaltic cones and flows range in age from ~0.02 to 1.95 Ma (Turrin and Dohrenwend, 1984), and the distribution of these ages (as estimated from relative morphologic degradation and calibrated by K-Ar ages) indicates an abrupt slowing of volcanic activity at ~0.75 Ma. The flows, as much as 6.1 km long and 1.9 km wide, also occur as 2 distinct morphologic types. Elongate flows at Lunar Crater are characterized by L/W ratios generally >4, by mean surface gradients ranging between 1.5% and 5%, and by flow thicknesses of 3 to 5 m. In contrast to Cima, most of the elongate flows at Lunar Crater that are suitable for drainage analysis are large (>2 km^2). Equant flows are characterized by L/W ratios <3, by mean surface gradients <2.5%, and by flow thicknesses of 5 to as much as 25 m. As in the case of Cima, the areas of equant flows vary significantly.

The Lunar Crater area is subject to an arid, continental climate. The mean minimum January temperature is –8 °C, the mean maximum July temperature is 32 °C, and the mean annual temperature is approximately 11 °C. The 12 cm of mean annual precipitation is typically almost uniformly distributed throughout the year (U.S. Department of Commerce, 1965). Mean annual temperatures during the late Pleistocene in the central Great Basin are estimated to have been as much as 7 °C colder (Dohrenwend, 1984), and mean annual precipitation was probably not substantially greater than at present (Spaulding and others, 1983). The sparse vegetation on the Lunar Crater lava flows is predominantly that of a sagebrush steppe where species of *Artemisia* are the dominant shrub and perennial grasses make up most of the understory (Young and others, 1977).

Flow Surface Degradation

The surfaces of the youngest flows in both fields are unstable, highly irregular, and extremely permeable (Fig. 2). Original constructional relief is generally <5 m on the younger elongate flows and as much as 10 m on younger equant flows. Constructional forms include pressure ridges, leveed lava channels, collapse depressions, digitate margins, and interlobe depressions and valleys. These constructional forms have significantly influenced initial stages of drainage development. Older flow surfaces

Figure 2. Rough, unstable, highly permeable surface of a 0.015-m.y.-old lava flow in the Cima volcanic field. Modification of the original flow surface has been limited to slight rubbling of topographic highs and partial infilling of topographic lows with colluvial rubble and eolian fines.

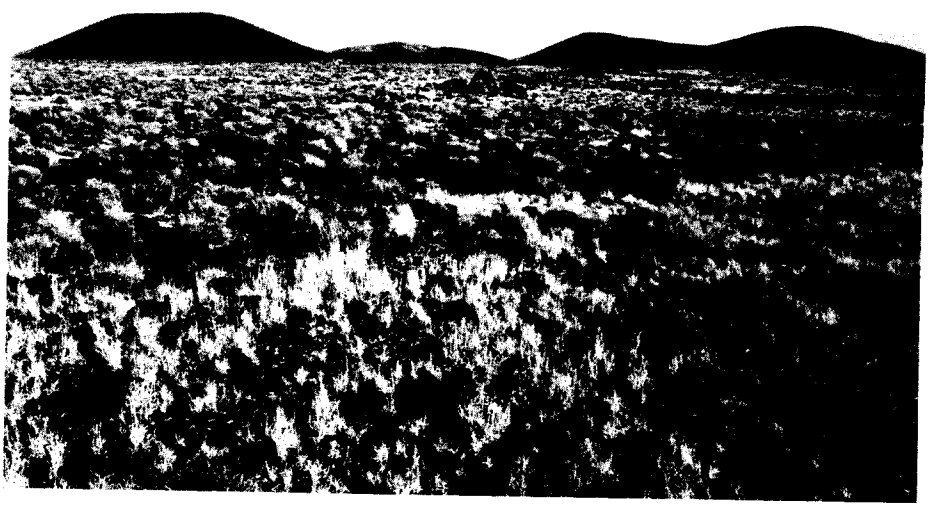

Figure 3. Interlocking stone pavements and widely scattered, profoundly degraded constructional forms distinguish the surface of this 0.53 ± 0.10-m.y.-old flow in the Lunar Crater volcanic field.

are comparatively flat, relatively featureless, and impermeable (Figs. 3 and 4). Constructional relief on these flows, where present, is generally <2 m, and drainage networks on these older flows appear to be largely unaffected by original constructional form.

Degradation of lava-flow surfaces in both fields is largely controlled by the entrapment of eolian silt and fine sand and the subsequent development of soils within these accreting eolian mantles (Wells and others, 1985; McFadden and others, 1986). Flows younger than 0.25 m.y. old are undergoing reduction of surface relief by eolian burial, constructional form rubbling, and local colluviation; flow surfaces between 0.25 and ~0.75 m.y. old are relatively flat and stable; and flows older than ~0.75 m.y. are dominated by surface runoff and fluvial erosion processes. These temporal variations in flow-surface form and process largely result from soil development within the eolian mantle. Soils on flows younger than 0.25 m.y. old are weakly developed with thin cambic B horizons and Stage I to I+ calcic horizons; moderately developed soils with argillic B horizons and Stage II to III calcic horizons occur on 0.25- to 0.70-m.y.-old flows; and strongly developed soils with argillic B horizons engulfed by secondary carbonate and Stage III calcic horizons are present on 0.70- to 1.1-m.y.-old flows (McFadden and others, 1986). This progressive soil development reduces flow surface permeability, thereby enhancing surface runoff processes (Wells and others, 1985). Subsequent fluvial erosion strips the eolian mantle and associated soils from flow surfaces and eventually exposes the massive interiors of the flows. Thus, the drainage networks on these lava flows have formed in response to accumulation of eolian mantles of silt and fine sand and to soil development within these eolian veneers, and the slow operation of these processes fosters the slow development of these networks. This slow rate of development provides an ideal opportunity for studying the earlier stages of drainage-network evolution.

Drainage Networks

The drainage networks developed on the accretionary mantles of the Cima and Lunar Crater lava flows increase in complexity with increasing flow age (Fig. 5). Drainage on younger flows is largely controlled by original flow morphology. These drainages are typically subparallel with low link frequencies and drainage densities. In contrast, constructional control is not apparent on most of the older flows; drainages are more nearly dendritic with relatively high link frequencies and drainage densities. On all flows, fingertip tributaries (exterior

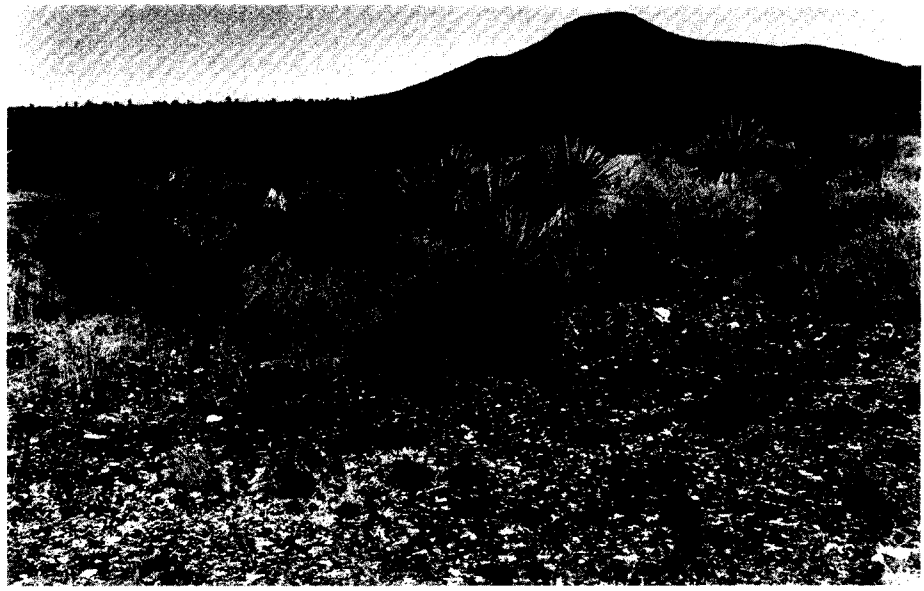

Figure 4. Gentle rounding, a paucity of constructional forms, and noninterlocking to interlocking stone pavements with abundant pedogenic carbonate rubble characterize the surface of this 0.85 ± 0.05-m.y.-old flow in the Cima volcanic field.

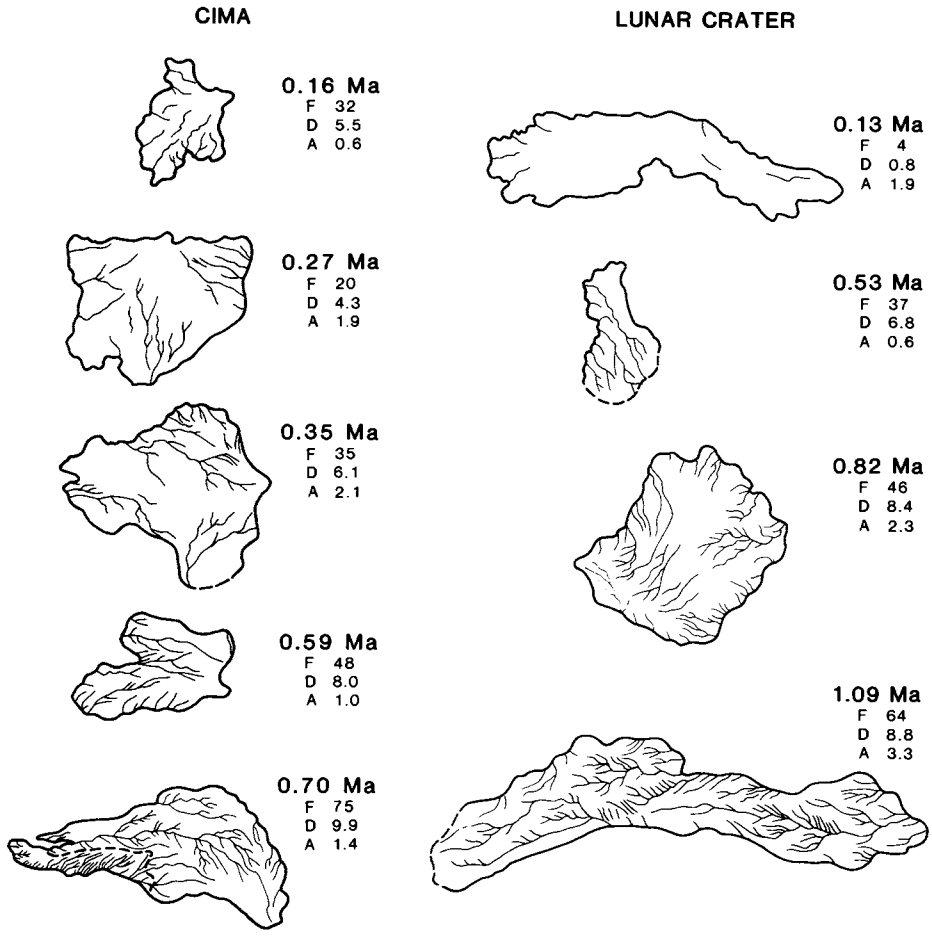

Figure 5. Drainage networks developed on K-Ar–dated lava flows in the Cima and Lunar Crater volcanic fields. F = link frequency; D = drainage density; A = flow-surface area.

links) are small and indistinct. Even the largest channels are typically less than a few metres wide and 1 m deep. Valleys are shallow, only locally cutting through the eolian mantle into the subjacent basalt.

Initiation of these channel networks has proceeded by means of two general mechanisms. (1) At some distance from flow margins, isolated channels have developed subparallel to the general flow direction, grown in length, possibly bifurcated, and eventually merged with other channels to form larger, more complex networks (Fig. 5). This mechanism is akin to that in the stream convergence simulation models of Leopold and Langbein (1962), Smart and others (1967), and Howard (1971). (2) Along flow margins, other channels have developed at high angles to the general flow direction, eroded headward, and in some cases, bifurcated and (or) merged with other channels. This mechanism is similar to that in the headward growth simulation models of Howard (1971), Smart and Moruzzi (1971), and Dunkerley (1977). Both mechanisms appear to operate to varying degrees on all flows; however, their relative importance seems to depend on flow size and shape, a composite measure of which is provided by the ratio of flow area to flow perimeter, A/P. In general, the stream convergence mechanism appears to be more important on the larger and more equant flows, where A/P is relatively large, whereas the headward growth mechanism appears to be more effective on the smaller and more elongate flows, where A/P is relatively small. This morphological effect significantly influences drainage-network development.

Figure 6. Changes in drainage-network parameters with increasing flow age (plotted on arithmetic axes). Black squares designate low-A/P flows (where A/P < 0.18); patterned circles, high-A/P flows (where A/P > 0.18). Solid curved lines represent estimated functional relations.

(A) Drainage density (D) versus flow age (t). D is measured in kilometres per square kilometre, and t is in millions of years before the present (Ma).

(B) Link frequency (F) versus flow age (t). F is measured in number per square kilometre.

(C) Mean link length ($\bar{l}$) versus flow age (t). $\bar{l}$ is measured in kilometres.

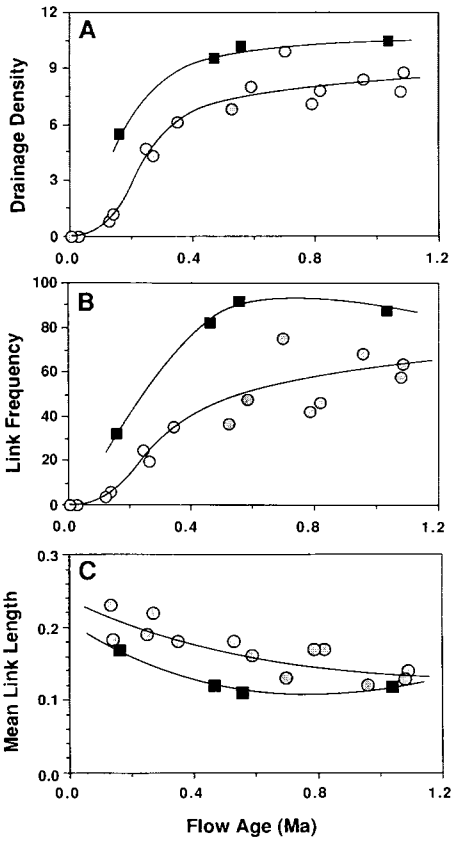

Although generally similar to conventional low-order drainage networks, drainage networks developed on the Cima and Lunar Crater lava flows differ from most other drainage systems in one significant respect. The degraded lava-flow surfaces are generally convex upward transverse to the general flow direction. As a consequence, the drainage networks on these surfaces include many small, isolated, and generally diverging drainage lines; the relations between drainage density and link frequency for these partly divergent networks are somewhat different from corresponding relations for convergent networks. Most notably, link frequencies are somewhat less for these divergent networks than what would be predicted for convergent networks with similar drainage densities.

MEASUREMENT OF DRAINAGE PARAMETERS

Lava flows suitable for analysis of drainage development must be carefully selected to minimize the variability of nontemporal influences

TABLE 1. CHARACTERISTICS OF DRAINAGE NETWORKS DEVELOPED ON BASALTIC LAVA FLOWS OF THE CIMA AND LUNAR CRATER VOLCANIC FIELDS

Flow age (m.y.)	Flow type	Flow area (km^2)	A/P*	L/W†	Slope (%)	Stream frequency (#/km^2)	Link frequency (#/km^2)	Drainage density (km/km^2)	Mean link length (km)	Kappa (κ)§	Percent ME** links (%)	Percent TS†† links (%)
Lunar Crater volcanic field												
0.02 ± 0.02	Equant	4.15	.30	2.8	2.6	0	0	0.0	..	..	..	..
0.13 ± 0.07	Elongate	1.92	.23	6.4	1.6	4	4	0.8	0.23	5.32	71	0
0.53 ± 0.10	Equant	0.62	.20	2.4	2.3	31	37	6.8	0.18	0.80	20	26
0.79 ± 0.14	Elongate	2.38	.29	3.8	5.0	39	42	7.1	0.17	0.84	36	12
0.82 ± 0.06	Equant	2.28	.37	1.8	1.8	39	46	7.8	0.17	0.74	40	24
0.96 ± 0.10	Equant	0.56	.19	1.8	2.5	57	68	8.4	0.12	0.97	30	33
1.08 ± 0.15	Elongate	6.31	.36	4.3	4.4	43	58	7.7	0.13	0.98	27	48
1.09 ± 0.08	Elongate	3.30	.29	7.3	5.0	48	64	8.8	0.14	0.83	21	42
Cima volcanic field												
0.01 ± 0.005	Elongate	1.00	.20	6.4	2.9	0	0	0.0	..	..	..	..
0.14 ± 0.05	Elongate	0.94	.20	4.3	3.3	6	6	1.1	0.18	4.84	20	0
0.16 ± 0.07	Equant	0.60	.17	2.5	6.0	32	32	5.5	0.17	1.04	65	0
0.25 ± 0.05	Equant	0.73	.22	2.4	4.2	25	25	4.7	0.19	1.10	40	0
0.27 ± 0.05	Equant	1.93	.32	1.6	7.8	18	20	4.3	0.22	1.06	29	11
0.35 ± 0.04	Equant	2.05	.32	2.0	7.4	28	35	6.1	0.18	0.94	13	27
0.47 ± 0.05	Elongate	0.68	.16	5.4	5.2	66	82	9.6	0.12	0.90	29	29
0.56 ± 0.08	Elongate	0.61	.15	3.9	2.9	80	92	10.2	0.11	0.88	36	18
0.59 ± 0.12	Equant	0.97	.20	2.4	5.5	42	48	8.0	0.16	0.77	36	24
0.70 ± 0.06	Elongate	1.47	.24	3.8	5.1	55	75	9.9	0.13	0.77	13	47
1.04 ± 0.07	Elongate	1.12	.15	10.1	4.6	80	88	10.4	0.12	0.81	53	15

*Ratio of flow-surface area to flow perimeter.
†Ratio of flow length to flow width.
§Shreve's kappa equals link frequency divided by the square of the drainage density.
**Marginal exterior.
††Tributary source.

on drainage development. Suitable flows should be situated on gently sloping, largely undissected surfaces within areas of relative tectonic stability. The surfaces of these flows should be free from modification by streams arising in areas external to the flow and by significant burial with alluvial fan deposits or with either air-fall or flow-rafted tephra. In addition, flow-surface areas should be sufficiently large (>0.50 km^2) to reduce the effects of drainage development along flow margins.

On the basis of these criteria, 10 K-Ar–dated lava flows in the Cima volcanic field and 7 K-Ar–dated flows in the Lunar Crater volcanic field were selected for analysis of drainage-network development. In addition to these 17 flows, the youngest flow at each field (although devoid of drainage lines) was also included in the analysis to facilitate study of the earliest stages of drainage development. Morphometric and drainage-network data for these 19 lava flows were obtained primarily from photogeologic mapping and topographic map measurements. These analyses were supported by field-based observations. Selected lava flows and their associated drainage networks were mapped on 1/20,000 nominal-scale, natural-color aerial photographs at Cima and on 1/24,000 color infrared and 1/35,000 panchromatic aerial photographs at Lunar Crater. This mapping was transferred to 1/24,000 U.S. Geological Survey topographic maps (with either 20-ft, 40-ft, or 10-m contour intervals). Flow morphometry (including flow area, perimeter length, and average length, width, and surface gradient) and drainage-network characteristics (link counts and link lengths) were measured from these annotated topographic maps. To verify these data, drainage lines were counted on 1- to 2-km field transects across selected flow surfaces at both fields. Close correspondence between these field transect counts and the photogeologic data and consistency of the drainage networks mapped on the two different types and scales of aerial photography at Lunar Crater indicate the overall accuracy of the photogeologic data.

DRAINAGE DEVELOPMENT

Morphologic and drainage-network data for the Cima and Lunar Crater lava flows are summarized in Table 1. These data show several related and progressive changes with flow age (Figs. 5 through 11). After 0.1 to 0.2 m.y., the time required for accumulation of nearly continuous eolian mantles across flow surfaces, drainage networks begin to form. Drainage density (D) and link frequency (F) increase, and mean link length ($\bar{l}$) decreases, first rapidly and then progressively more slowly with increasing flow

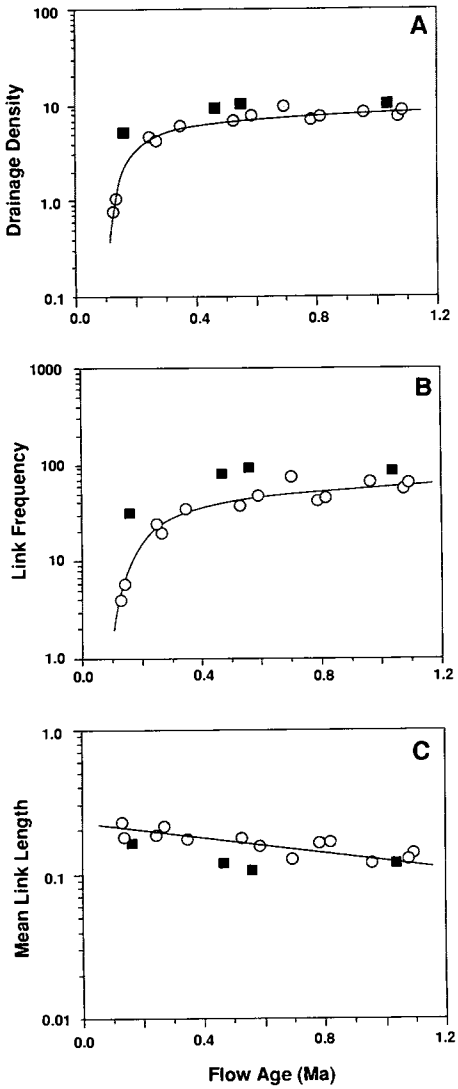

Figure 7. Changes in drainage-network parameters (plotted on logarithmic axes) with increasing flow age. Black squares designate low-A/P flows (where A/P < 0.18); patterned circles, high-A/P flows (where A/P > 0.18). The solid curved lines in Figures 7A and 7B represent estimated functional relations for the high-A/P flows. The solid straight line in Figure 7C is the reduced major axis for the high-A/P flows.

(A) Drainage density (D) versus flow age (t). D is measured in kilometres per square kilometre, and t in Ma. For t > 0.4 Ma, logD = 0.82 + 0.10t.

(B) Link frequency (F) versus flow age (t). F is measured in number per square kilometre. For t > 0.4 Ma, logF = 1.44 + 0.35t.

(C) Mean link length ($\bar{l}$) versus flow age (t). $\bar{l}$ is measured in kilometres. The reduced major axis is log$\bar{l}$ = –0.63 – 0.25t, r^2 = 0.67, p = 0.0007.

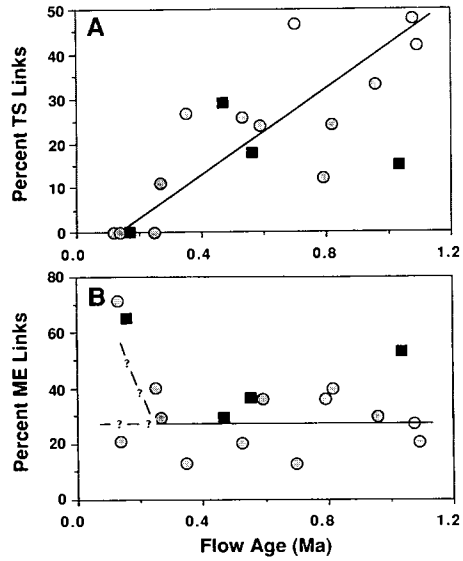

Figure 8. Changes in the proportions of exterior link lengths with increasing flow age. Black squares designate low-A/P flows (where A/P < 0.18); patterned circles, high-A/P flows (where A/P > 0.18).

(A) Tributary source link percent (%TS) versus flow age (t). The reduced major axis is %TS = –6.92 + 49.7t, r^2 = 0.63, p = 0.0013.

(B) Marginal exterior link percent (%ME) versus flow age (t). Where t > 0.2 Ma, there is no significant relation between %ME and t.

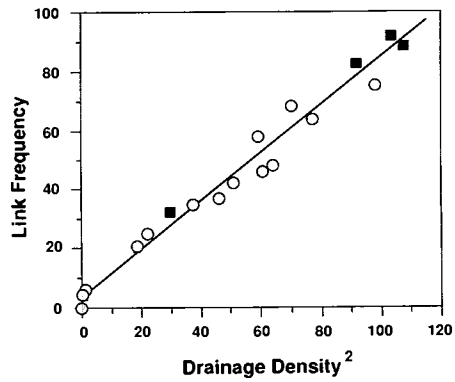

Figure 9. Changes in link frequency (F) with increasing drainage density squared (D^2), plotted on arithmetic axes. Black squares designate low-A/P flows (where A/P < 0.18); patterned circles, high-A/P flows (where A/P > 0.18). The regression equation for this relation is F = 3.5 + 0.80D^2, r^2 = 0.98, p = 0.0001. Because of the high coefficient of determination, this equation approximates the functional relation between F and D^2.

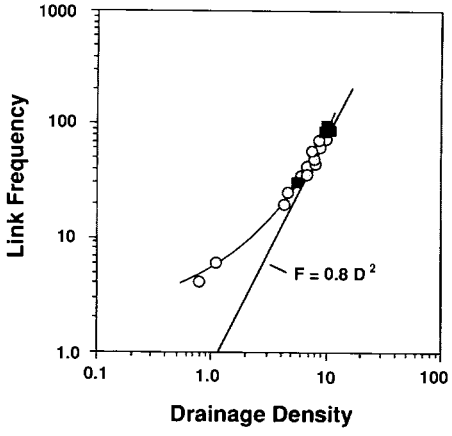

Figure 10. Changes in link frequency (F) with increasing drainage density (D), plotted on logarithmic axes. Black squares designate low-A/P flows (where A/P < 0.18); patterned circles, high-A/P flows (where A/P > 0.18). On this plot, the relation between F and D approximates a smooth curve that may be viewed as the evolutionary path followed by a developing drainage network on one of the Cima or Lunar Crater lava flows.

TABLE 2. DRAINAGE NETWORK DEVELOPMENT ON LAVA FLOWS OF THE CIMA AND LUNAR CRATER VOLCANIC FIELDS

Parameters	Regrssion equation	r^2	N	p
D versus t, all flows*	$D = -0.47 + 32.7t - 14.4t^2$	0.85	19	0.0001
D versus t, high A/P*	$D = -0.74 + 21.7t - 12.6t^2$	0.94	15	0.0001
F versus t, all flows*	$F = -5.8 + 162t - 89.6t^2$	0.69	19	0.0001
F versus t, high A/P*	$F = -4.9 + 119t - 53.1t^2$	0.88	15	0.0001
$\bar{l}$ versus t, all flows*	$\bar{l} = 0.22 - 0.17t + 0.08t^2$	0.52	17	0.006
$\bar{l}$ versus t, high A/P*	$\bar{l} = 0.23 - 0.12t + 0.03t^2$	0.73	13	0.001
F versus D^2, all flows	$F = 3.5 + 0.80D^2$	0.98	19	0.0001
Fs versus D^2, all flows	$Fs = 4.1 + 0.65D^2$	0.95	19	0.0001

Note: regression equations are between drainage network parameters and flow age. D = drainage density; t = flow age; A = flow-surface area; P = flow perimeter; F = link frequency; $\bar{l}$ = man link length; Fs = stream frequency.

*Although these regressions demonstrate the strong influence of time on drainage network development, they are not suitable approximations of the functional relations between these data and time. Approximate functional relations have been estimated by eye and are presented in Figures 6 and 7.

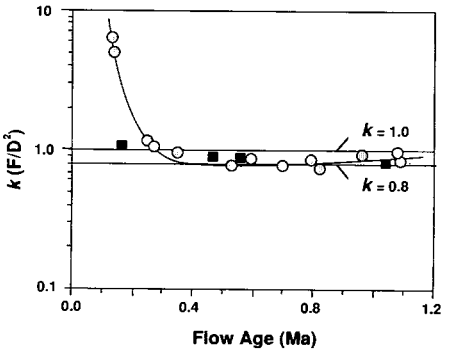

Figure 11. Plot of Shreve's κ (= F/D^2) against flow age (t). The solid curved line represents the estimated functional relation for the high-A/P flows. Where $0 < t < 0.2$, κ decreases rapidly; where $0.2 < t < 0.5$, κ decreases more slowly to a minimum value of ~0.75; and where $t > 0.5$, κ increases slowly toward 1.0 in accordance with $\log\kappa = -0.2 + 0.15t$.

age (t) (Fig. 6). On flows older than ~0.4 m.y. D and F attain a condition of approximate adjustment, increasing slowly in a manner such that logD and logF increase at nearly constant rates (Fig. 7) and κ (= F/D^2) increases slowly toward 1 from a minimum value of ~0.75 (Fig. 11). These changes are statistically significant (Table 2) and apply generally to all of the flows studied.

If it is assumed that these changes with flow age reflect changes through time, they indicate that these drainage networks grow in a manner that is consistent with the qualitative model of Glock (1931). An initial period of elongation, lasting for ~0.2 to 0.3 m.y., extends master drainages to all parts of a flow. Elaboration then replaces elongation as the principal mode of network extension and remains predominant throughout the remainder of the 1.1-m.y. period of record. Elaboration proceeds primarily by the addition of short tributaries to existing streams and secondarily by the formation of short isolated streams along flow margins.

Effect of Flow Morphology

Drainage density, link frequency, and mean link length are significantly affected by the size and shape of the Cima and Lunar Crater lava flows. On flows of similar age, D and F are consistently higher and $\bar{l}$ is consistently lower on low-A/P flows (where A/P < 0.18) than on high-A/P flows (where A/P > 0.18). Of these parameters, D shows the least sensitivity to flow morphology and is the most consistently related to flow age (Fig. 6A, Table 2). D is still significantly affected by flow size and shape, however. On older flows, D averages 25% higher on low-A/P flows than on high-A/P flows, and the correlation between D and t is stronger for high-A/P flows than for all flows (Table 2). In comparison to D, F is more strongly affected by flow morphology and less consistently related to flow age (Fig. 6B, Table 2). On older flows, F is ~60% higher on low-A/P flows than on high-A/P flows, and the correlation between F and t is substantially stronger for high-A/P flows than for all flows (Table 2). Changes in mean link length ($\bar{l}$) are clearly related to changes in D and F (Fig. 6C). The slow and progressively decreasing rate of change in $\bar{l}$ is predicted by the definition of mean link length, $\bar{l}$ = D/F, and the empirical relation, $F \propto D^2$, which together require that $\bar{l} \propto 1/D$. Consequently, $\bar{l}$ is also significantly affected by flow morphology, averaging 10% to 30% less on low-A/P flows than on high-A/P flows.

That D and F are significantly higher on low-A/P-ratio flows than on high-A/P-ratio flows is a reflection of the relative concentration of small drainage channels along flow margins, which seem to be locally favorable sites for channel development. The net result is that both D and F are generally higher around flow edges than near the centers of flows. This "edge effect" has influenced drainage development on all flows, but it is particularly pronounced on the smaller, more elongate flows where P is large relative to A. Consequently, drainage networks on flows that have low A/P ratios tend to have higher values of D and F and lower values of $\bar{l}$. This effect significantly increases the scatter of data in Figure 6 and blurs the shape of the D-t, F-t, and $\bar{l}$-t relations. To avoid this problem, the data for the 4 flows where A/P is <0.18 are plotted using a different symbol in all figures, and these data are disregarded in determining the functional relations between variables. Functional relations that appear to be linear have been estimated by the reduced major axis, as no information is available regarding the error variances of the drainage-network parameters. Functional rela-

tions that are nonlinear have been estimated by eye, as the data scatter is generally small and the relations do not conform to any conventional curvilinear functions.

Changes in Network Parameters with Flow Age

If plotted in semi-logarithmic space (Fig. 7), the D-t and F-t relations for drainage networks on high-A/P lava flows are remarkably similar in shape to the relations obtained by Leopold and others (1964, p. 425) for drainage networks on glacial till sheets in Iowa. In both instances, D and F increase first rapidly and then more slowly, the change in the rate of increase in D being more pronounced than the change in the rate of increase in F.

Although it is not obvious from the scatter of data in Figure 7 that D and F continue to increase for cases where $t > 0.4$ Ma, this interpretation is consistent with the inverse linear relation between $\log\bar{l}$ and t (Fig. 7C). Because $\bar{l} = D/F$,

$$\frac{d\log\bar{l}}{dt} = \frac{d\log D}{dt} - \frac{d\log F}{dt} \qquad (5)$$

and Figure 7 shows that where $t > 0.4$ Ma, $d\log D/dt \simeq 0.10$, $d\log F/dt \simeq 0.35$, and $d\log\bar{l}/dt \simeq -0.25$. These values satisfy equation 5 and support the validity of the interpretation that D and F continue to increase slowly where $t > 0.4$ Ma.

The tendency for D and F to increase and for $\bar{l}$ to decrease on these older flows can be attributed to the process of network elaboration. This process involves the formation and growth of exterior links along existing streams (termed "tributary source," TS, links) and along flow margins (termed "marginal exterior," ME, links). On flows older than 0.2 Ma, the proportion of TS links to total exterior links shows a general and continuing increase with flow age (Fig. 8A), whereas the proportion of ME links to total exterior links remains essentially unchanged (Fig. 8B). Thus, it is evident that the continuing addition of TS links is largely responsible for the continuing increase in D and F and the continuing decrease in $\bar{l}$ on flows older than 0.4 Ma.

The Link Frequency–Drainage Density Relation

Link frequency is very strongly related to drainage density ($r^2 = 0.98$), according to the relation $F = 3.5 + 0.80D^2$ (Fig. 9, Table 2). As D increases, this relation approximates

$$F = 0.8D^2 \qquad (6)$$

which is somewhat different from the relation developed by Shreve (1967), $F = D^2$ (equation 4). This discrepanccy can be traced to the fact that the drainage networks on the Cima and Lunar Crater lava flows include many exterior links that either drain off flow margins or are not connected to larger drainages. The creation of each of these "isolated" exterior links increases the number of links in the drainage network by one, whereas the creation of an exterior link that joins a larger drainage (a TS link) also involves the creation of an additional interior link and increases the number of links by two. Consequently, F is sensitive to the proportion of isolated exterior links within the network, and the value of F for a given value of D should be less than what is predicted by equation 4.

The F-D relation for young, developing networks is emphasized if D and F are plotted using logarithmic coordinates. On a logarithmic plot, these data approximate a smooth curve that may be viewed as an evolutionary path followed by a developing drainage network (Fig. 10). All but the two youngest flows plot close to the approximate relation $F = 0.8D^2$, suggesting that drainage networks approach a condition of approximate adjustment between the number and total length of channel links very early in their evolution. The departure of the youngest flows from the relation predicted by equation 6 is perhaps best explained by rewriting this equation as

$$\bar{l} = (1.25\ A/N)^{0.5} \qquad (7)$$

where N is the number of links developed on a flow of area A. For the flows analyzed in this study (for which $A > 0.5$ km^2), this relation predicts that if drainage development starts with the formation of a single stream channel, the initial link should be several times longer than the actual links which have developed on the youngest flows. In point of fact, drainage on these flows apparently starts with the more or less simultaneous development of several short and generally divergent channels which still tend to be substantially shorter than predicted by equation 7.

This evolutionary adjustment between F and D is portrayed even more clearly in a semi-logarithmic plot of κ ($= F/D^2$) against t (Fig. 11). During the earliest stages of network development, κ greatly exceeds the values predicted by either equation 4 or 6. As the networks grow, κ declines rapidly and reaches a minimum value of ~0.75 after ~0.4 to 0.5 m.y. (at about the same time that the rates of change in logD and logF become approximately constant). Thereafter, as these networks evolve toward maximum extension, κ increases slowly as required by the relative rates of change in D and F with time. Rewriting equation 2 in logarithmic form and differentiating,

$$\frac{d\log\kappa}{dt} = \frac{d\log F}{dt} - \frac{2\ d\log D}{dt}, \qquad (8)$$

and recalling that $d\log F/dt \simeq 0.35$ and $d\log D/dt \simeq 0.10$ where $t > 0.4$ Ma (Fig. 7), it follows that $d\log\kappa/dt \simeq 0.15$. Kappa may not reach the expected value of 1 for converging drainage networks, however, because 25% to 30% of the exterior links are ME links that drain off flow margins. Consequently, even at maximum extension, the value of F for a given value of D is likely to be less than predicted by equation 4 so that the value of κ ($= F/D^2$) is likely to be < 1.

CONCLUSIONS

Drainage networks on the basaltic lava flows of the Cima and Lunar Crater volcanic fields show progressive differences that are strongly linked to flow age. If it is assumed that these spatial differences reflect temporal changes, they provide useful insights into the early development of drainage networks.

(1) Drainage-network development has proceeded at about the same rate on lava flows in the Cima and Lunar Crater volcanic fields. Drainage densities and link frequencies for morphologically comparable flows in both fields increase at about the same rate and reach maximum values at approximately the same time. These nearly identical rates of drainage development reflect the highly similar geologic, physiographic, and climatic environments on lava flows in these two fields.

(2) Drainage development on the Cima and Lunar Crater lava flows proceeds very slowly. The ~1-m.y. period required to approach a condition of maximum extension is more than an order of magnitude longer than the time required for the development of mature drainage networks on glacial till in central Iowa (Leopold and others, 1964, p. 425) or on the lacustrine plains of Pleistocene Lake Lahontan in the Black

Rock Desert of northwestern Nevada (J. C. Dohrenwend, unpub. data). This slow rate of network growth is primarily due to a close linkage between the establishment of surface drainage on these lava flows and the gradual reduction in flow surface permeability induced by eolian mantle accretion and subsequent soil development within this accretionary mantle. The self-enhancing feedback mechanisms that effect extension of the developing drainage networks on these eolian mantles are largely constrained by these slow, progressive processes. As a result, drainage development proceeds very slowly, thus creating an ideal situation for studying developing drainage networks.

(3) Drainage networks on the Cima and Lunar Crater lava flows are strongly affected by flow size and shape. Drainage densities and link frequencies attain maximum values 25% to 60% larger on flows with low A/P ratios than on flows with high A/P ratios. This morphologic influence, largely owing to the relative concentration of small channels along flow margins, tends to obscure the pattern of drainage development. When this influence is removed, a pattern emerges that is essentially consistent with the phases of network extension described by Glock (1931).

(4) Drainage development appears to have followed the same general sequence on nearly all of the Cima and Lunar Crater lava flows. Surface drainage does not appear generally until large areas of the flow surface are buried beneath an accretionary mantle of eolian silt and fine sand (a process requiring 0.1 to 0.2 m.y.). Following accumulation of this eolian mantle and formation of a moderately developed soil within it, drainage development proceeds in a manner similar to that of the qualitative model proposed by Glock (1931). Elongation first extends master drainages to all parts of a flow, and D and F increase rapidly. After approximately 0.4 m.y., elaboration replaces elongation as the principal mode of network extension. Elaboration proceeds by the addition of tributaries to master drainages and by formation of short "isolated" drainages along flow margins. D and F continue to increase but more slowly and in a manner such that logD and logF increase at nearly constant rates. These trends continue throughout the remainder of the 1.1-m.y. period of record as the networks evolve toward maximum extension. Because drainage development is largely confined to the thin (2–5 m) accretionary mantle and to the uppermost part of the subjacent flow, channels remain shallow, valley widening is limited, and continued network development proceeds slowly.

(5) The evolutionary adjustment between D and F is perhaps most clearly portrayed by the change in the value of κ with flow age. This change approximates a smooth curve that may be viewed as an expression of the evolutionary path followed by a developing network. Because drainage initiation apparently occurs with the more or less simultaneous development of several short and generally diverging channels, κ greatly exceeds 1 during the earliest stages of network development. As the network grows, however, κ declines rapidly and reaches a minimum value of ~0.75 after ~0.4 to 0.5 m.y. (at about the same time that the rates of change in logD and logF become approximately constant). With continued drainage development, κ increases slowly toward 1, the expected equilibrium value for convergent networks. However, because a substantial proportion of the network's exterior links continue to drain directly off flow margins, it is unlikely that κ will reach the value of 1 as predicted for converging drainage networks.

REFERENCES CITED

Dohrenwend, J. C., 1984, Nivation landforms in the western Great Basin and their paleoclimatic significance: Quaternary Research, v. 22, p. 275–288.

Dohrenwend, J. C., McFadden, L. D., Turrin, B. D., and Wells, S. G., 1984a, K-Ar dating of the Cima volcanic field, eastern Mojave Desert, California: Late Cenozoic volcanic history and landscape evolution: Geology, v. 12, p. 163–167.

Dohrenwend, J. C., Wells, S. G., Turrin, B. D., and McFadden, L. D., 1984b, Rates and trends of late Cenozoic landscape degradation in the area of the Cima volcanic field, eastern Mojave Desert, California, *in* Dohrenwend, J. C., ed., Surficial geology of the eastern Mojave Desert, California: Geological Society of America 1984 Annual Meeting, Reno, Nevada, Guidebook, p. 101–115.

Dunkerley, D. L., 1977, Frequency distributions of stream link lengths and the development of channel networks: Journal of Geology, v. 85, p. 459–470.

Glock, W. S., 1931, The development of drainage systems: A synoptic view: Geographical Review, v. 21, p. 475–482.

Howard, A. D., 1971, Simulation of stream networks by headward growth and branching: Geographical Analysis, v. 3, p. 29–50.

Leopold, L. B., and Langbein, W. B., 1962, The concept of entropy in landscape evolution: U.S. Geological Survey Professional Paper 500-A, 20 p.

Leopold, L. B., Wolman, M. G., and Miller, J. P., 1964, Fluvial processes in geomorphology: San Francisco, California, W. H. Freeman and Company, 522 p.

Luedke, R. G., and Smith, R. L., 1978, Map showing distribution, composition, and age of late Cenozoic volcanic centers in Arizona and New Mexico: U.S. Geological Survey Miscellaneous Geologic Investigations Map I-1090-A, scale 1:1,000,000.

——1981, Map showing distribution, composition, and age of late Cenozoic volcanic centers in California and Nevada: U.S. Geological Survey Miscellaneous Geologic Investigations Map I-1090-C, scale 1:1,000,000.

McFadden, L. D., Wells, S. G., and Dohrenwend, J. C., 1986, Influences of Quaternary climatic changes on processes of soil development on desert loess deposits of the Cima volcanic field, California: Catena, v. 13, p. 361–389.

Melton, M. A., 1958a, Geometric properties of mature drainage systems and their representation in an E_4 phase space: Journal of Geology, v. 66, p. 35–54.

——1958b, Correlation structure of morphometric properties of drainage systems and their controlling agents: Journal of Geology, v. 66, p. 442–466.

Morisawa, M. E., 1964, Development of drainage systems on an upraised lake floor: American Journal of Science, v. 262, p. 340–354.

Parker, R. S., 1977, Experimental study of drainage basin evolution and its hydrologic implications: Colorado State University Hydrology Paper 90, 51 p.

Parker, R. S., and Schumm, S. A., 1982, Experimental study of drainage networks, *in* Bryan, R., and Yair, A., eds., Badland geomorphology and piping: Norwich, England, Geo Books, p. 153–168.

Ruhe, R. V., 1952, Topographic discontinuities of the Des Moines lobe: American Journal of Science, v. 250, p. 46–56.

Schumm, S. A., 1956, Evolution of drainage systems and slopes in badlands at Perth Amboy, New Jersey: Geological Society of America Bulletin, v. 67, p. 597–646.

——1977, The fluvial system: New York, Wiley-Interscience, 352 p.

Shreve, R. L., 1967, Infinite topologically random channel networks: Journal of Geology, v. 75, p. 178–186.

Smart, J. S., and Moruzzi, V. L., 1971, Computer simulation of Clinch Mountain drainage networks: Journal of Geology, v. 79, p. 572–584.

Smart, J. S., Surkan, A. J., and Considine, J. P., 1967, Digital simulation of channel networks: International Association of Scientific Hydrology, International Union of Geodesy and Geophysics, Symposium on River Morphology, 14th, p. 87–98.

Spaulding, W. G., Leopold, E. B., and Van Devender, T. R., 1983, Late Wisconsin paleoecology of the American southwest, *in* Porter, S. C., ed., Late Quaternary environments of the United States, Volume 1, The late Pleistocene: Minneapolis, Minnesota, University of Minnesota Press, p. 259–293.

Turrin, B. D., and Dohrenwend, J. C., 1984, K-Ar ages of basaltic volcanism in the Lunar Crater volcanic field, northern Nye County, Nevada: Implications for Quaternary tectonism in the central Great Basin: Geological Society of America Abstracts with Programs, v. 16, no. 6, p. 679.

Turrin, B. D., Dohrenwend, J. C., Drake, R. E., and Curtis, G. H., 1985, K-Ar ages from the Cima volcanic field, eastern Mojave Desert, California: Isochron/West, no. 44, p. 9–16.

U.S. Department of Commerce (Weather Bureau), 1955, Climatic summary of the United States—Supplement for 1931 through 1952, California: Climatography of the United States No. 11-4, p. 94, 118, 129.

——1965, Climatic summary of the United States—Supplement for 1951 through 1960, Nevada: Climatography of the United States No. 86-22, p. 9, 27, 31.

Vasek, F. C., and Barbour, M. G., 1977, Mojave Desert scrub vegetation, *in* Barbour, M. G., and Major, J., eds., Terrestrial vegetation of California: New York, Wiley-Interscience, p. 835–868.

Wells, S. G., Dohrenwend, J. C., McFadden, L. D., Turrin, B. D., and Mahrer, K. D., 1985, Late Cenozoic landscape evolution on lava flow surfaces of the Cima volcanic field, Mojave Desert, California: Geological Society of America Bulletin, v. 96, p. 1518–1529.

Young, J. A., Evans, R. A., and Major, J., 1977, Sagebrush steppe, *in* Barbour, M. G., and Major, J., eds., Terrestrial vegetation of California: New York, Wiley-Interscience, p. 763–796.

MANUSCRIPT RECEIVED BY THE SOCIETY APRIL 7, 1986
REVISED MANUSCRIPT RECEIVED FEBRUARY 27, 1987
MANUSCRIPT ACCEPTED MARCH 7, 1987

Printed in U.S.A.